Materials Science-Poland, 34(4), 2016, pp. 741-746
http://www.materialsscience.pwr.wroc.pl/
DOI: 10.1515/msp-2016-0109

DE GRUYTER OPEN

Synthesis and study of structural properties of Sn doped ZnO nanoparticles

M. ARSHAD JAVID[1]*, M. RAFI[1], IHSAN ALI[2], FAYYAZ HUSSAIN[3], M. IMRAN[3], ALI NASIR[4]

[1]Department of Basic Sciences (Physics), University of Engineering & Technology, Taxila, Pakistan
[2]Government Municipal Postgraduate College, Toba Tek Singh, Pakistan
[3]Department of Physics, Bahudin Zikria University, Multan, Pakistan
[4]Department of Mechanical Engineering, UET, Taxila, Pakistan

Pure and Sn-doped ZnO nanostructures were synthesized by simple chemical solution method. In this method we used zinc nitrate and NaOH as precursors. Sn doping content in ZnO was taken with the ratio 0, 5, 10, 15 and 20 percent by weight. Physical properties of Sn-doped ZnO powder were studied by XRD analysis which revealed that Sn doping had a significant effect on crystalline quality, grain size, intensity, dislocation density and strain. The calculated average grain size of pure ZnO was 21 nm. The best crystalline structure was found for 0 wt.%, 5 wt.% and 10 wt.% Sn doping as observed by FESEM and XRD. However, higher Sn-doping (>10 wt.%) degraded the crystallinity and the grain size of 27.67 nm to 17.76 nm. The structures observed in FESEM images of the samples surfaces were irregular and non-homogeneous. EDX depicted no extra peak of impurity and confirmed good quality of the samples.

Keywords: *nanoparticles; chemical solution method; physical properties; XRD analysis*

1. Introduction

Zinc oxide is a type of semiconductor material having band gap of 3.37 eV and high binding energy of 60 MeV. ZnO materials are used in solar cells, UV detectors, gas sensors and photo catalysts, because of good optical, optoelectronic and piezoelectric properties [1]. ZnO properties can be improved using different techniques [2, 3]. ZnO is an excellent nanoscale metal oxide. ZnO is an n-type II – VI semiconductor having normally a hexagonal or wurtzite structure. ZnO microstructure has found novel applications in gas sensors, solar cells, varistors and photocatalyst with high chemical activity [4–7]. ZnO based improvements have been made on nanomaterials in basic sciences and advanced material engineering [8, 9]. Sn is an active n-type dopant in ZnO. The radius of Sn^{+4} (0.071 nm) is almost equivalent to Zn^{+2} (0.074 nm) which is favorable in substituting Zn ions in ZnO lattice in order to adjust visible emission of ZnO materials by Sn-doping [10–12]. Sn doped ZnO was successfully synthesized and its physical and chemical properties were studied [13]. The improvement of zinc oxide properties has been proposed by the refinement of its nanostructure and optimizing its morphology [14, 15].

Different synthesis techniques of ZnO particles have been reported [16–20]. In this work, we synthesized the Sn doped ZnO nanoparticles using chemical solution method. XRD, FESEM and EDX analyses have been carried out.

2. Experimental

2.1. Synthesis of Sn doped ZnO nanoparticles

Sn doped ZnO nanoparticles have been synthesized using a simple chemical solution method. The stock solutions of starting materials 50 mM zinc nitrate $Zn(NO_3)_2{\cdot}2H_2O$, 50 mM stannic chloride $SnCl_4{\cdot}5H_2O$ and 100 mM sodium hydrate

*E-mail: arshad.javid@uettaxila.edu.pk

NaOH were prepared using deionized water as a solvent for each sample. The solution of NaOH was dropped into the solution of $Zn(NO_3)_2{\cdot}2H_2O$ under continuous magnetic stirring till the formation of white precipitates of $Zn(OH)_2$. The precipitates were filtered off and washed with distilled water for five times. The precipitates of $Zn(OH)_2$ were first dried in air at room temperature and then heated at 250 °C for 24 hours to attain fine crystallinity. For the preparation of 5 wt.%, 10 wt.%, 15 wt.% and 20 wt.% Sn doped zinc oxide, the stock solutions of 50 mM $Zn(NO_3)_2{\cdot}2H_2O$ and 50 mM $SnCl_4{\cdot}5H_2O$ were mixed accordingly to each composition and the same procedure as used for the preparation of ZnO was adopted for each case.

The synthesized samples were characterized using a Rigaku XRD instrument with monochromatic CuKα radiation source having wavelength of 1.5418 Å. The morphology studies and compositional analysis of nanoparticles were carried out by FESEM integrated with EDX (TIMA3 LM TESCAN). The samples were coated with carbon using low voltage sputtering and then analyzed under SEM operating at a voltage of 20 kV.

3. Results and discussion

3.1. Structural parameters

Fig. 1a shows the XRD patterns of ZnO with 0 % Sn concentration. The X-ray diffraction patterns of samples a, b and c are consistent with the reference codes 01-005-0664 and 01-075-0576. The peak with (h k l) value (1 0 1) positioned at 36.36° has maximum intensity. The (1 0 1) major plane along with some other minor planes indicate the polycrystalline nature of the prepared material having hexagonal geometry [21, 22].

When the Sn doping of ZnO material increased above 10 wt.%, the intensity of the major peak has increased showing the improvement in the crystallinity [23]. Beyond 10 wt.% Sn doping, the decrease in intensity of the major peak corresponding to (0 1 5) plane has been observed what indicates poor crystallinity. Sn doping has improved the crystallinity up to the concentration level of 10 wt.% but ZnO crystal structure showed poor crystallinity above the Sn concentration level of 10 wt.%.

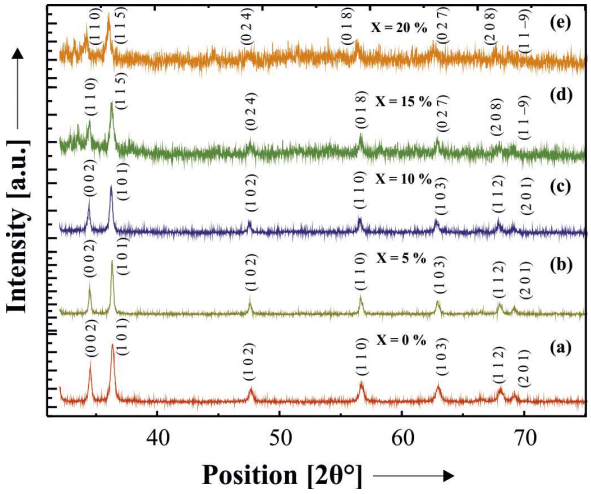

Fig. 1. X-ray diffraction peaks of 0 wt.%, 5 wt.%, 10 wt.%, 15 wt.% and 20 wt.% Sn doped zinc oxide.

The grain sizes of the prepared samples were calculated using Debye-Scherrer's formula [24]:

$$d = \frac{K\lambda}{\beta \cos\theta} \tag{1}$$

where d is the grain size, k is a constant taken to be 0.89 for the hexagonal structure, λ is the wavelength of X-ray used (1.5418 Å), β is full width at half maximum and θ is the Bragg's angle. Equation 1 is multiplied by a factor π/180 to change the value of W from degree to radian:

$$d = \frac{K\lambda}{\beta \cos\theta} \cdot \frac{\pi}{180} \tag{2}$$

Table 1. Variation of grain size with the increase of Sn content in $Zn_{1-x}Sn_xO$ (x = 0.00 to 0.20) [33]

x	2θ	FWHM	Intensity [a.u.]	Grain size [nm]
0.00	36.2	0.006671	679.96	21.3270
0.05	36.2	0.005137	814.26	27.663
0.10	36.2	0.00521	377.49	25.272
0.15	36.2	0.00676	122.60	21.028
0.20	36.2	0.0080	71.8320	17.763

The calculated average grain size of pure ZnO is 21 nm and it decreases up to 17 nm for 20 wt.% Sn-doped sample. The variation in grain size with the

increase in Sn concentration is shown in Fig. 2 and Table 1. The grain size decreases with Sn content which is likely due to the substitution of Sn metal into zinc oxide lattice [25, 26].

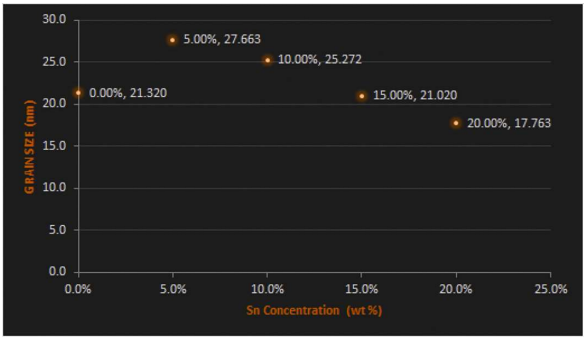

Fig. 2. Grain size versus Sn content of ZnO nanoparticles.

The strain produced in the samples due to Sn doping has been calculated using the relation [27]:

$$€ = \frac{\beta \cos\theta}{4} \tag{3}$$

where € is strain and θ is the Bragg's angle in degrees.

Dislocation density was calculated by [28]:

$$\delta = \frac{1}{d^2} \tag{4}$$

The dislocation density (δ), defined as the length of dislocations lines per unit volume has been estimated using equation 4.

Table 2. Calculation of strain, and dislocation density with an increase of Sn content in $Zn_{1-x}Sn_xO$ (x = 0.00 to 0.20).

x	Strain (€)	Grain size [nm]	Dislocation density (δ) [lines/m^2]
0.00	0.001584	21.3270	0.00212
0.05	0.00122	27.663	0.00130
0.10	0.00123	25.272	0.00161
0.15	0.0016	21.028	0.00226
0.20	0.0019	17.763	0.00317

Calculated values of strain and dislocation density are presented in Table 2.

The effect of strain in ZnO nanoparticles due to Sn dopant is demonstrated by the grain size (d), strain (€), and dislocation density (δ) given in Table 2. For the samples with Sn-doping concentration of 5 wt.%, the grains tend to increase in size because of the small strain in the sample that influences the normal growth of ZnO. However, when Sn-doping concentration is 10 wt.%, the grain size slightly decreases because of higher strain. This shows again that the best crystalline structure is achieved only up to 10 wt.% Sn doping as previously followed from XRD analysis. At higher doping up to 10 wt.%, the grain size decreases again as a result of greater stress leading to poor crystallinity. It should be mentioned that the strain value (€) depends on both β and cosθ as shown in equation 3. Dislocation density (δ) may also be considered as a measure of crystallinity. Among the different doping concentrations 5 wt.% and 10 wt.% doping give the smallest (δ) which shows the best crystalline structure compared to higher or lower doped ones [29].

The microstructure and morphology of nanoparticles were analyzed using FESEM. Fig. 2 shows the micrographs of the samples of Sn doped ZnO nanoparticles. The images show clearly the morphological changes due to the different doping levels of Sn in ZnO. The Sn doped ZnO nanoparticles are inhomogeneous in nature. Interestingly, when we increase the doping rate, the morphological changes of the microstructure show the mechanism of nucleation and/or wrinkles growth [30]. These variations are produced by Sn atoms which promote the growth of network-winkles destressing the microstructure and reducing energy of the system. Similar result was presented by Bahsi et al. [31] in the study of the effect of Mn and Cu doping on microstructure of ZnO. Furthermore, the surface micrographs showed that the doping of Sn plays an important role in changing and improving the structure of the ZnO nanoparticles. The ratio of Sn is the main factor that controls the morphology and structure of the final product. This may be due to the defects created by Sn doping. The size of these crystalline structures varies in the range

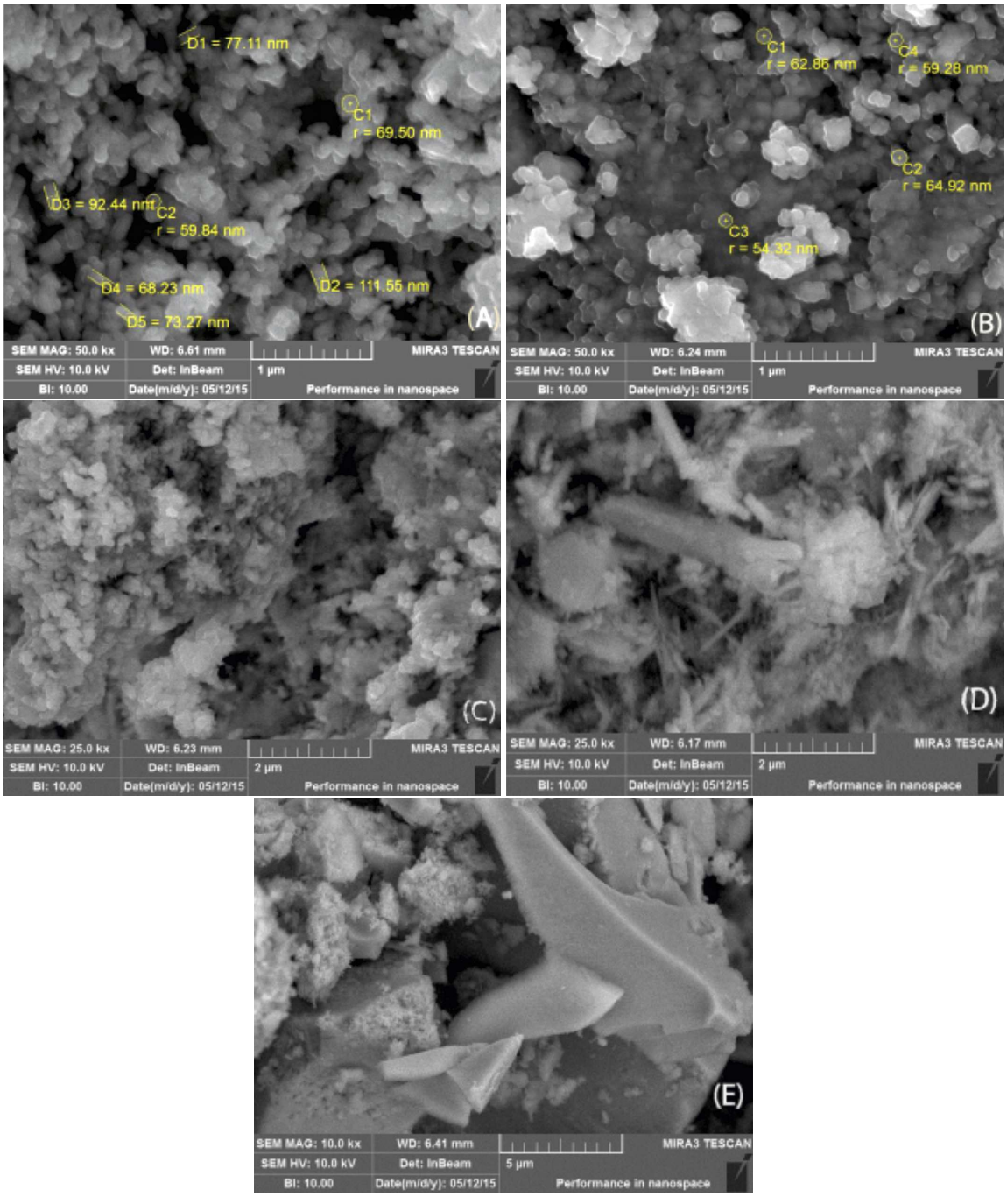

Fig. 3. FESEM micrographs for different concentrations of Sn doped ZnO nanoparticles (A) 0 wt.%; (B) 5 wt.%; (C) 10 wt.%; (D) 15 wt.%; (E) 20 wt.%.

of ∼54 nm to 111 nm in Fig. 3A and Fig. 3B. When the concentration of Sn dopant increased from 5 wt.% to 10 wt.%, the Sn-doped ZnO nanoparticles showed noticeable variations in the surface morphology [32]. Anisotropic growth of crystal results from the driving force of the dopant on ZnO lattice, hence, Sn-doped ZnO nanostructures have a granular shape as shown in Fig. 3A to Fig. 3C. Furthermore, ZnO nanoparticles at higher Sn concentrations (above 10 wt.%), (Fig. 3D and

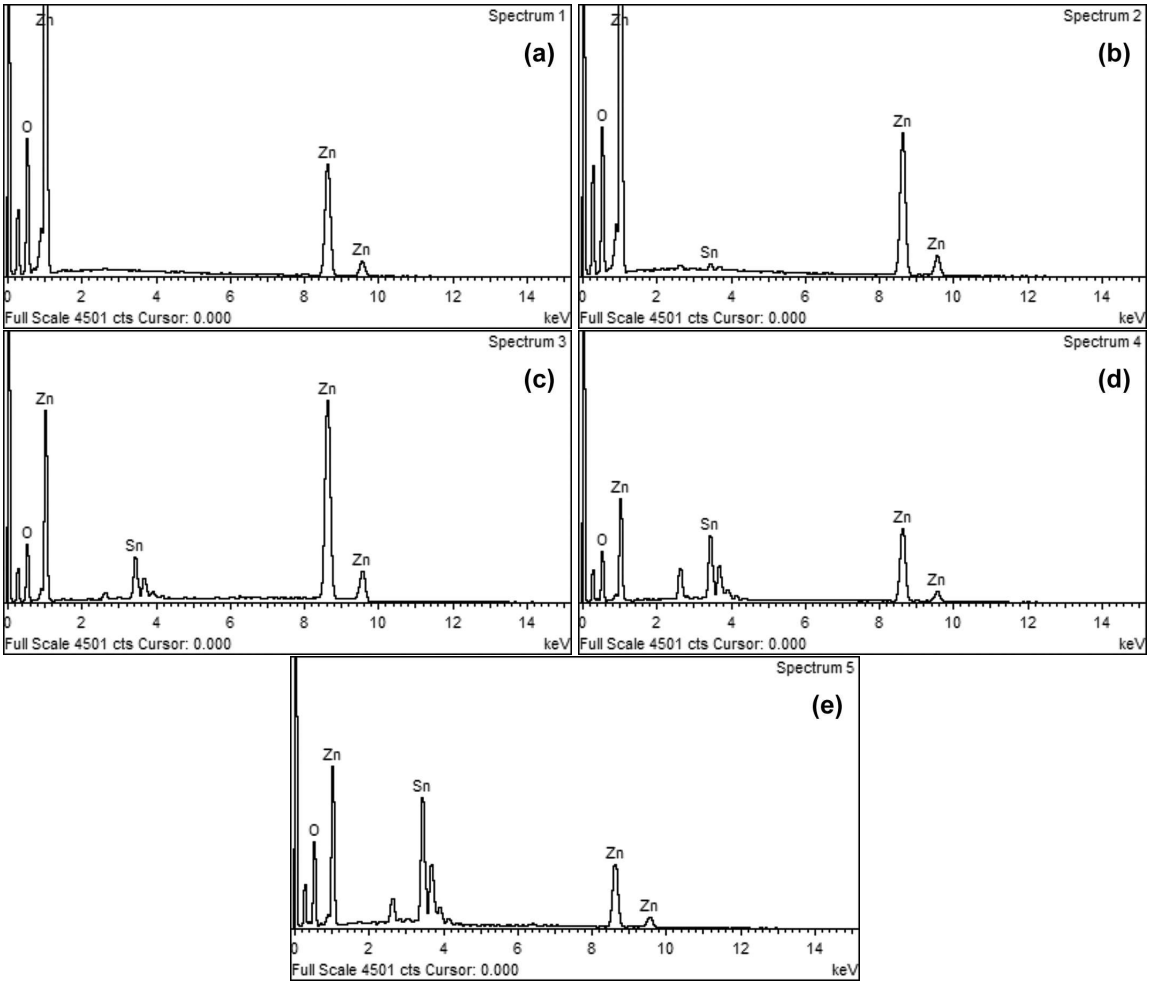

Fig. 4. EDX spectra of ZnO nanoparticles doped by different concentrations of Sn (a) 0 wt.%; (b) 5 wt.%; (c) 10 wt.%; (d) 15 wt.%; (e) 20 wt.%.

Fig. 3E) tend to agglomerate and show irregular flake structure [32].

EDX analysis was carried out to study the quality and composition of Sn-doped ZnO nanostructured samples [33]. EDX analysis confirmed the presence of Zn, O and Sn elements in the synthesized materials. Fig. 4a shows the spectrum of pure ZnO with two to three high intense peaks which are associated with Zn and O atoms.

The measured atomic percentage of these elements is about 42.04 and 57.96, respectively. Fig. 4b and Fig. 4d exhibit the results of EDX analysis of Sn-doped ZnO nanoparticles; the measured Sn contents are 0.52, 3.27, 8.03 and 9.68 atomic percentage, respectively, for the four nominal compositions of 5 wt.%, 10 wt.%, 15 wt.% and 20 wt.%, indicating that Sn percentage in the ZnO nanoparticles increases according the nominal loading of Sn [33, 34]. Results of elemental analysis of ZnO doped by different concentrations of Zn are compared in Table 3.

4. Conclusions

Sn doped ZnO nanoparticles have been synthesized using a simple chemical solution method. The average grain size of pure ZnO is 21 nm and it decreases up to 17 nm for the sample doped with 20 wt.% Sn. The increased Sn concentration results in the agglomeration which has taken place. XRD results show that the material is polycrystalline with preferred orientations (1 0 1) and (0 1 5).

Table 3. Compositional analysis of synthesized Sn doped ZnO nanoparticles at 0 wt.%, 5 wt.%, 10 wt.%, 15 wt.% and 20 wt.%.

	ZnO – 0 % Sn		ZnO – 5 % Sn		ZnO – 10 % Sn		ZnO – 15 % Sn		ZnO – 20 % Sn	
Element	[wt.%]	[at.%]	[wt.%]	[at.%]	[wt.%]	[at.%]	[wt.%]	[at.%]	[wt.%]	[at.%]
Zn	74.77	42.04	75.09	43.86	82.89	65.63	57.70	37.93	39.34	22.21
O	25.23	57.96	23.31	55.62	9.61	31.10	20.12	54.04	29.53	68.12
–	–	–	1.61	0.52	7.49	3.27	22.18	8.03	31.13	9.68
Total	100	100	100	100	100	100	100	100	100	100

It is observed that up to 10 wt.% Sn doping, the peak intensity corresponding to plane (1 0 1) increases and thus the grain size increases, while for Sn concentration above 10 wt.%, the peak intensity decreases which indicates poor crystallinity of the samples. FESEM results show the fine granular structure for 0 and 5 wt.% Sn doping in ZnO. The structure has been disturbed above the Sn doping level of 10 wt.% that might be due to the incorporation of excessive amount of Sn metal into the crystal structure of ZnO materials.

References

[1] LI G., HU G.G., ZHOU H.D., FAN X.J., LI X.G., *Mater. Chem. Phys*., 75 (2002), 101.

[2] MIURA K., MASUDA M., ITOH M., HORIKAWA T., MACHIDA K.I., *J. Alloy. Compd.*, 408 (2006), 1391.

[3] HUANG S., WANG L., LIU L., HOU Y., LI L., *Agron. Sustain. Dev.*, 35 (2015), 369.

[4] GONCHAR A., GORELIK S., KATYNKINA S., LETYUK L., RYABOV I., *J. Magn. Magn. Mater.*, 215 (2000), 221.

[5] HUANG J., ZHUANG H., LI, W., *Mater. Res. Bull*., 38 (2003), 149.

[6] PEREIRA F.M.M., SANTOS M.R.P., SOHN R.S., ALMEIDA J.S., MEDEIROS A.M.L., *J. Mater. Sci.-Mater. El.*, 20 (2009), 408.

[7] CHO H.S., KIM S.S., *IEEE T. Magn.*, 35 (1999), 3151.

[8] NEDKOV I., PETKOV A., KARPOV V., *IEEE T. Magn.*, 26 (1990), 1483.

[9] SHEN G., XU M., XU Z., *Mater. Chem. Phys.*, 105 (2007), 268.

[10] SUGIMOTO S., HAGA K., KAGOTANI T., INOMATA K., *J. Magn. Magn. Mater.*, 290 (2005), 1188.

[11] ALI I., ISLAM M.U., AWAN M.S., AHMAD M., *J. Alloy. Compd.*, 547 (2013), 118.

[12] BATOO K.M., KUMAR S., LEE C.G., *Curr. Appl. Phys.*, 9 (2009), 826.

[13] PIRES G.F.M., RODRIGUES H.O., ALMEIDA J.S., SANCHO E.O., GOES J.C., COSTA M.M., DENARDIN J.C., SOMBRA, A.S.B., *J. Alloy. Compd.*, 493 (2010), 326.

[14] FISTER M.J., DE GEUS A., RHINES W.C., HU J., CASSIDY R., *IEEE T. Nucl. Sci.*, 43 (1996), 2874.

[15] KOOPS C.G., *Phys. Rev*., 83 (1951), 121.

[16] REDDY M.B., REDDY P.V., *J. Appl. Phys*., 75 (1994), 6125.

[17] WATAWE S.C., SARWADE B.D., BELLAD S.S., SUTAR B.D., CHOUGULE B.K., *J. Magn. Magn. Mater.*, 214 (2000), 55.

[18] TSAKALOUDI V., KOGIAS G., ZASPALIS V.T., *J. Alloy. Compd*., 588 (2014), 222.

[19] REZLESCU N., REZLESCU E., *Phys. Status Solidi A*, 23 (1974), 575.

[20] PILLAI P.K.C., *Polymeric Electrets*, Plastics Engineering, New York, 1995.

[21] OUNNUNKAD S., WINOTAI P., *J. Magn. Magn. Mater*., 301 (2006), 292.

[22] BSOUL I., MAHMOOD S.H., *J. Alloy. Compd.*, 489 (2010), 110.

[23] LECHEVALLIER L., LE J.M., BRETON J.F., HARRIS I.R., *J. Magn. Magn. Mater*., 269 (2004), 192.

[24] LEE S.W., AN S.Y., SHIM I.B., KIM C.S., *J. Magn. Magn. Mater*., 290 (2005), 231.

[25] IQBAL M.J., ASHIQ M.N., GUL I.H., *J. Magn. Magn. Mater*., 322 (2010), 1720.

[26] EL ATA A.A., REICHA F.M., ALI M.M., *J. Magn. Magn. Mater*., 292 (2005), 17.

[27] SAWADH P.S., KULKARNI D.K., *B. Mater. Sci*., 24 (2001), 47.

[28] JIA L., LUO J., ZHANG H., XUE G., JING Y., *J. Alloy. Compd*., 489 (2010), 162.

[29] KUMAR M.P, SHANKARAPPA T., KUMAR B.V., NAGARAJA N., *Solid State Sci.*, 11 (2009), 214.

[30] IQBAL M.J., ASHIQ M.N., *Chem. Eng. J.*, 136 (2008), 383.

[31] BAHSI Z.B., ORAL A.Y., *Opt. Mater.*, 29 (2007), 672.

[32] MOTT N.F., DAVIS E.A., *Electronic Processes in Non-Crystalline Materials*, Clarendon Press, London, 1979.

[33] PRAKASH T., JAYAPRAKASH R., ESPRO C., NERI G.,KUMAR E.R.,, *J. Mater. Sci.*, 49 (2014), 1776.

[34] SIRDESHMUKH L., KUMAR K.K., LAXMAN S.B., KRISHNA A.R., SATHAIAH G., *B. Mater. Sci.*, 21 (1998), 219.

Received 2015-12-27
Accepted 2016-09-24